# Ion-beam induced amorphization and dynamic epitaxial recrystallization in α-quartz

Sankar Dhar, Wolfgang Bolse, and Klaus-Peter Lieb

**Articles you may be interested in**

# Ion-beam induced amorphization and dynamic epitaxial recrystallization in $\alpha$-quartz

Sankar Dhar, Wolfgang Bolse,[a)] and Klaus-Peter Lieb[b)]

*II. Physikalisches Institut and Sonderforschungsbereich 345, Universität Göttingen, Bunsenstr. 7-9, D-37073 Göttingen, Germany*

We report on the evaluation of ion-beam induced damage in $\alpha$-quartz and its dynamic annealing behavior in the temperature range between 80 and 1050 K using Rutherford backscattering spectrometry in channeling geometry. The results illustrate that the critical temperature for inhibiting amorphization during irradiation is about $T_c \approx 940$ K. The critical fluence $\phi_c$ for amorphization is independent of the temperature up to 550 K, but strongly increases at higher temperatures. The activation energy for the diffusion of defects in the collision cascade or at the amorphous/crystalline interface is found to be $0.28 \pm 0.02$ eV. The dynamic annealing mechanism is explained by the vacancy out-diffusion model of Morehead and Crowder. © *1999 American Institute of Physics.* [S0021-8979(99)03006-6]

## I. INTRODUCTION

$SiO_2$ is one of the key materials for various photoelectronic applications such as high density optical storage, broadband photonic communication, etc., apart from its traditional use as an electrical insulator in Si based devices.[1,2] Ion implantation is indispensable in several processing steps for making such devices or structures but it induces radiation damage. The accumulation of radiation damage is intentional in many applications such as to change the refractive index for making wave guides[3] but in other cases[4] its recovery is essential. Thus, it is very important to understand both the basic mechanisms of accumulation of damage and its dynamic annealing behavior at elevated irradiation temperatures. Until now, various studies have been performed in order to understand the mechanism and microstructure of radiation damage in $\alpha$-quartz and its transformation into amorphous phase at low temperature.[5–8] However, the knowledge of the temperature dependence of ion-beam induced damage formation and its dynamic annealing behavior and how it is related to the various ion processing parameters (i.e., flux, fluence, implanted species, etc.) still need to be developed. For the past few years, various methods based on thermal, ion beam, etc., techniques have been successfully developed to epitaxially recover the radiation damage in single-crystal substrates[9] but have not been applied successfully in $\alpha$-quartz.[10,11] Only recently,[12] solid phase epitaxial regrowth (SPEG) of ion-beam amorphized single-crystal $\alpha$-quartz by thermal annealing has been found after alkali implantation and annealing in oxygen atmosphere. This discovery of SPEG, which until now has been regarded as an unachievable process,[10,11] has also raised the possibility of epitaxial recovery by other methods. The interest in ion-beam induced epitaxial growth (IBIEG) is due to the low temperatures involved in the recrystallization process compared to thermal annealing technique.[9] For studying damage recovery by the IBIEG process, the prerequisite knowledge of various parameters such as the critical temperature, the temperature dependence of critical fluence for amorphization, etc., is essential. In this article, we seek to understand the basic mechanisms and determine the parameters related to the dynamic annealing of ion-beam induced damage in $\alpha$-quartz at elevated temperature.

## II. EXPERIMENTAL PROCEDURES

For the present investigation, high quality single-crystal $\alpha$-quartz (0001) substrates, 10 mm×10 mm×1 mm in size and procured from CRYSTAL GmbH, were irradiated with 50 keV $^{20}$Ne ions at temperatures ranging from 80 to 975 K and fluences between $1\times10^{13}$ and $4\times10^{15}$ ions/cm$^2$. In order to prevent the sample temperature from further rising during irradiation, the ion flux was kept at about $1\times10^{13}$ ions/cm$^2$ s. The samples were mounted on a copper target holder connected to a resistive heater and equipped with thermocouples. The accuracy of the temperature measurement is estimated around $\pm 3$ K. During irradiation, half of the sample surface was covered with an Al foil in order to preserve an unmodified area needed for sample orientation during channeling analysis. An electrostatic X-Y beam sweep system was used to achieve homogeneous irradiations over an area of 1 cm$^2$.

The depth distributions of the damage introduced during implantation was determined at room temperature by means of Rutherford backscattering spectrometry combined with channeling (RBS-C), using the 15 nA 900 keV He$^{2+}$ beam. Both the irradiation and RBS-C measurements were carried out at the Göttingen heavy ion implanter IONAS.[13] A two-axes goniometer and a surface barrier detector of 14 keV resolution full width at half maximum (FWHM) placed at an angle 165° were used for the analyses. In order to avoid charging by the beam, the sample edges were covered by

---

a)Present address: Institut für Strahlenphysik, Universität Stuttgart, Allmandring 3, 70569 Stuttgart, Germany.

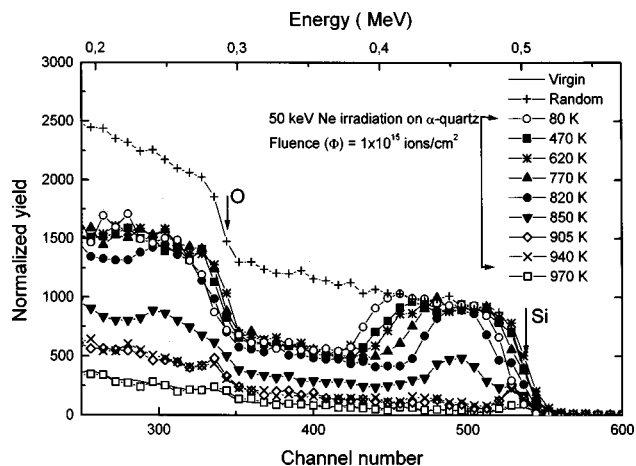b)Author to whom correspondence should be addressed; electronic mail: lieb@up2002.dnet.gwdg.de

FIG. 1. RBS-C spectra of $\alpha$-quartz samples before and after 50 keV Ne$^+$ ion irradiations at a fluence of $1\times10^{15}$ ions/cm$^2$ and the different temperatures indicated.
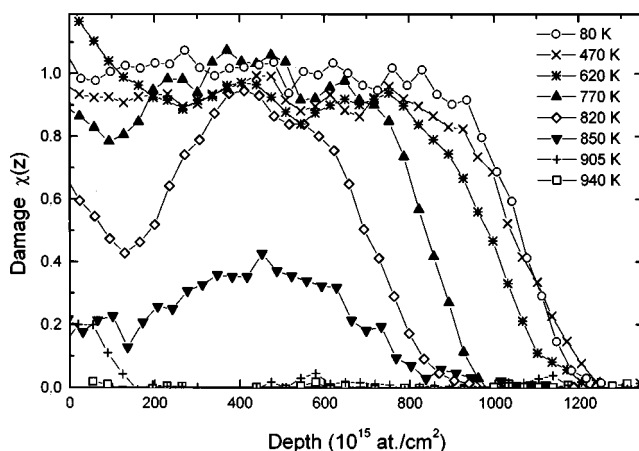


FIG. 2. The depth distributions of the irradiation damage $\chi(z)$ as obtained from the RBS-C spectra of Fig. 1.

conducting Ag paste. The apparent damage distribution was determined by means of the computer code DAMAGE, which is based on an algorithm given by Walker and Thompson[14] and allowed us to properly treat the dechanneled fraction of the analyzing $\alpha$ beam. The ion range and the damage energy density distribution $F_D$ were calculated using the TRIM95 code.[15]

## III. RESULTS AND DISCUSSIONS

### A. Ion-beam induced damage distribution

Figure 1 depicts the RBS-C spectra of a virgin sample in $\langle 0001 \rangle$ channeling and random orientations (the latter taken by rotating the sample azimuthally around an axis tilted 7° from the channeling direction). The surface positions of the Si and the O signal are indicated by arrows. In the near-surface region, a minimum channeling yield of 5% was found. The samples which were irradiated with 50 keV Ne ions at a fluence of $1\times10^{15}$ ions/cm$^2$ and at temperatures in the range of 80–620 K are also shown in Fig. 1. The RBS signal due to implanted Ne ions is not visible in the spectra because of the low fluence. At 80 K, the height of the RBS signals of both the Si and the O sublattice from the damage region near the surface reaches the random level indicating either the formation of a homogeneous amorphous layer or a region of randomly oriented crystallites embedded in an amorphous matrix. For constant ion fluence, the thickness of this disordered layer decreases with increasing temperature, indicating the competition between the effects of ion-beam induced amorphization and dynamic annealing. Above 900 K, only little damage remains in the sample and at 970 K the RBS-C spectrum is identical with that of the virgin sample.

The damage distributions $\chi(z)$ in the Si sublattice as a function of depth are illustrated in Fig. 2. At liquid nitrogen temperature, a coherent amorphous layer ($\chi=1$) of 135 nm thickness has formed which reduces at increasing temperatures. At about 800 K only a buried amorphous layer appears, while at temperatures above 850 K, the lattice becomes completely disordered. Above about 925 K, no measurable damage is produced in the sample at this Ne

fluence $(1\times10^{15}$ ions/cm$^2)$. The integrated damage [$I_X = \int \chi(z)dz$] as a function of temperature for two different fluences is shown in Fig. 3. At low temperatures almost no influence of the target heating can be observed, while at higher temperatures the integrated damage drops down within a relatively narrow temperature range, depending on the applied ion fluence. As already discussed above, no damage occurs any more for the sample irradiated with $1\times10^{15}$ ions/cm$^2$ at or above 940 K. Above this temperature, also further increase of the Ne fluence did not produce any considerable damage in the sample. Hence, the critical temperature at which irradiation-induced damage and dynamic thermal annealing compensate each other is about $T_c \approx 940$ K.

The normalized distribution $\chi(z,\phi)$ of the apparent damage generated at different temperatures and different irradiation fluences is independent of temperature and fluence, i.e., as long as coherent amorphous layers are not formed the shapes remain the same, as shown in Fig. 4. These distributions are also compared with the calculated damage energy profile $F_D(z)$[16] obtained from the TRIM95 simulation via $F_D(z)=E_d[2n_V(z)+n_D(z)]$, where $E_d=25$ eV is the displacement energy of quartz[17] and $n_D(z)$ and $n_V(z)$ denote
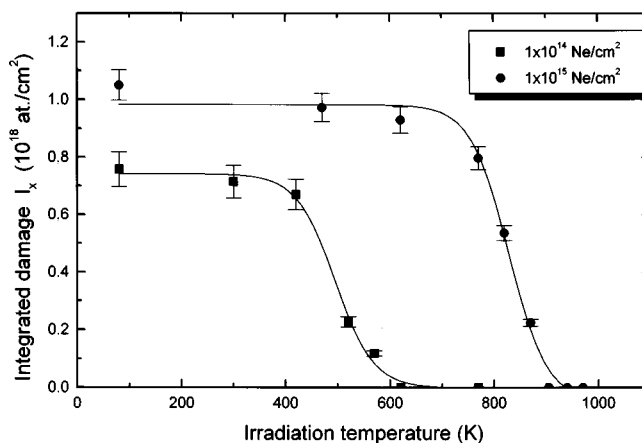


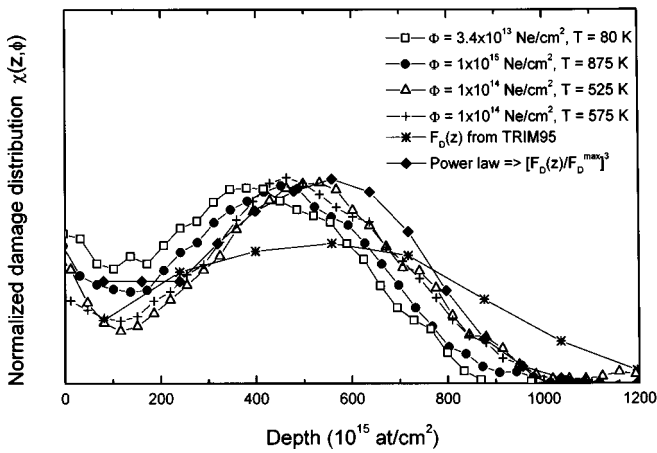FIG. 3. The integrated damage $I_x$ as a function of the irradiation temperature for two different fluences.

FIG. 4. Normalized damage distributions $\chi(z,\phi)$ as a function of depth. These results are compared with the calculated distribution obtained from the TRIM95 code, before and after scaling by a power function with the exponent $n=3$.



FIG. 5. The critical fluence $\phi_c$ is plotted as a function of irradiation temperature using Eq. (5). The fit corresponds to the parameters $E_a=0.28$ eV and $T_c=986$ K.

the numbers of displacement and replacement collisions, respectively. Evidently, the calculated distribution $F_D(z)$ does not fit the experimental profiles. However, recently a power law behavior of the apparent damage on the applied fluence has been observed in quartz and other ceramic materials[5,18] during low temperature ion bombardments which was attributed to the three-dimensional nucleation and growth of the amorphous phase. If we assume such a power law dependence, $\chi \sim (F_D(z)/F_D^{\max})^3$, we achieve good agreement with the data as shown in Fig. 4 in accordance with the previous results obtained at low temperature. The apparent damage due to the irradiation of $\alpha$-quartz could be described by the function[5]

$$\chi(\phi,z) = \left[ \frac{\phi \cdot F_D(z)}{\phi_c \cdot F_D^{\max}} \right]^n, \tag{1}$$

where $\phi_c$ is the critical fluence at which a coherent amorphous layer has formed, $F_D^{\max}$ is the deposited energy density in the maximum of the damage distribution and the exponent was found to about $n \approx 3$. This critical fluence obviously is a function of temperature, $\phi_c = \phi_c(T)$. Keeping in mind that according to Eq. (1) the integrated damage can be written as

$$\frac{I_X(\phi)}{I_X[\phi_c(T)]} = \left[ \frac{\phi}{\phi_c(T)} \right]^3, \tag{2}$$

we can estimate $\phi_c(T)$ from any damage distribution (below $\phi_c$), if we have information about $I_X(\phi_c)$, the integrated damage at the critical dose $\phi_c(T)$. In fact, since the shape of the normalized apparent damage distribution $\chi(z,\phi)$ is independent of temperature at $\phi < \phi_c$ (Fig. 4), the integrated damage $I_X(\phi_c)$ at the critical fluence $\phi_c(T)$ must be the same as for $T=80$ K, and we can calculate the critical fluences $\phi_c(T)$ using Eq. (2) for any damage distribution below $\phi_c$. As shown in Fig. 5, the values of $\phi_c$ are almost independent of temperature up to about 550 K and then start to increase strongly for increasing irradiation temperature. The critical temperature $T_c$ is the temperature at which $\phi_c$ goes to infinity and, as can be seen from Fig. 5, it is around 940 K, which is consistent with the results obtained from Fig. 3
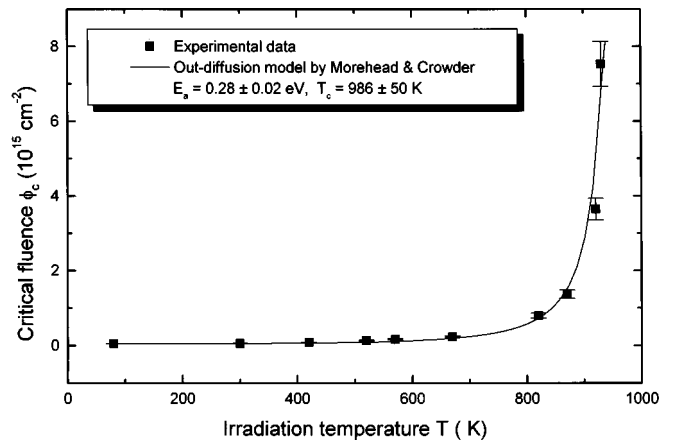
where we have shown that creation and annealing of damage compensate each other at about the same temperature.

## B. Mechanism of dynamic annealing

Low temperature ion-beam induced amorphization in materials, where dynamic annealing is suppressed, can be described in terms of the dense collision cascades initiated by the incident ions in the target and especially in quartz it is dominated by random nucleation and growth of local disordered regions.[5,19] At higher temperature, both amorphization and dynamic annealing occur simultaneously and the latter process starts dominating for increasing temperature. Only the vacancy out-diffusion model proposed by Morehead and Crowder[20] has been used to describe such a condition.

Morehead and Crowder in their vacancy out-diffusion model[20] assumed that the high vacancy density created at the core of the collision cascade diffuses towards the outer zones of the cascade at higher irradiation temperatures where the vacancies recombine with the interstitials. In this way, a less defective zone is formed in the outer region of the cascade volume and the radius of the heavily damaged inner zone shrinks with increasing temperature leaving less material in a disordered state. Consequently, the critical fluence $\phi_c(T)$ for amorphization increases with increasing temperature. Let $R_0$ be the radius of the damage region at low temperature where vacancy diffusion does not take place, and $\phi_c(0)$ be the corresponding critical fluence. If $R_0$ can be reduced by an amount of $\delta R(T)$ due to defect diffusion at higher temperature, the critical fluence $\phi_c$ can be written as

$$\frac{\phi_c(T)}{\phi_c(0)} = \frac{R_0^2}{(R_0 - \delta R)^2}. \tag{3}$$

The temperature dependence of $\delta R$ is governed by the Boltzmann-like behavior of the vacancy diffusivity

$$\delta R(T) = 2\sqrt{\tau D_v^o} e^{-(E_a/2k_B T)}, \tag{4}$$

where $D_v^o$ and $\tau$ are the vacancy diffusion constant and time and $E_a$ is the activation energy of the process. Rearranging Eqs. (3) and (4), we obtain
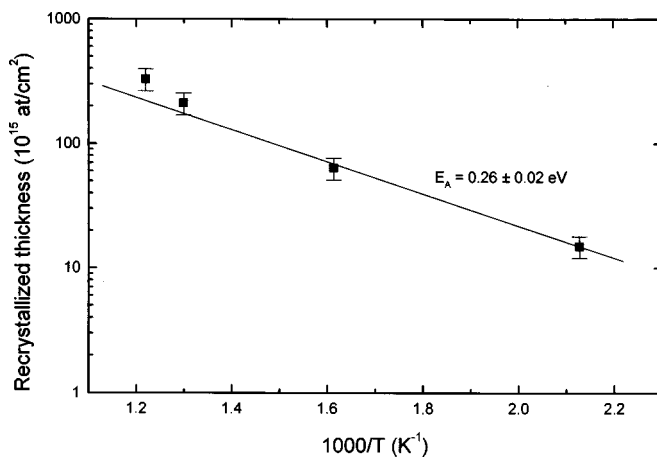
FIG. 6. The thickness of the recrystallized layer as a function of temperature.

$$\phi_c(T) = \phi_c(0)[1 - (L_0/R_0)e^{-(E_a/2k_BT)}]^{-2}. \quad (5)$$

$L_0 = 2\sqrt{D_v^0\tau}$ is the diffusion length at infinite temperature and the ratio $L_0/R_0$ is independent of temperature.

Figure 5 illustrates that the above function agrees well with the experimental data. The activation energy $E_a$ for the dynamic defect recovery becomes $E_a = 0.28 \pm 0.02$ eV. The critical temperature $T_c$ can be obtained from Eq. (5) by assuming $\phi_c(T_c)$ to be infinite. In this case, Eq. (5) is reduced to $T_c = E_a/2k_B \cdot \ln(L_o/R_o)$ and the deduced value of $T_c = 986 \pm 50$ K is very close to the present estimated experimental value of about 940 K. We should note here that these numbers are valid under the given irradiation conditions, i.e., for Ne ions at $\dot{\phi} = 1 \times 10^{13}$ ions/cm$^2$ s. In fact, the critical temperature and the activation energy depend on the ion species and flux. For example, $T_c$ has been found to increase with increasing ion mass. Experimental values of $T_c = 1446$ K and $E_a = 0.17$ eV in quartz were reported by Wang et al.[21] for Xe irradiations in SiO$_2$.

The decrease in thickness of the amorphous layer (see Figs. 1 and 2) with increasing temperature also follows an Arrhenius behavior, shown in Fig. 6. The value found for the activation energy of $E_A = 0.26 \pm 0.02$ eV agrees well with the activation energy $E_a = 0.28$ eV obtained for the diffusion of defects and suggests that the same annealing process is active below and above $\phi_c$. Similar observations were made in other materials. For example, in the case of InP, Wendler et al.[22] deduced $E_a = 0.35$ eV, either from the defect diffusion in the collision cascade or from the movement of the amorphous/crystalline interface. It may be noted that the activation energy obtained in the present case is similar to the one for viscous flow in quartz. The high activation energy for viscous flow is a signature of less susceptibility to amorphization under irradiation. This is the reason why Al$_2$O$_3$

cannot be amorphized due to its low activation energy of 0.014 eV for defect diffusion which is close to the activation energy for viscous flow.[21] For the same reason, quartz easily becomes amorphous under ion irradiation. Thus, there appears to exist a definite correlation between amorphization, defect annealing, and viscosity.

## IV. CONCLUSIONS

The present investigation on the amorphization and dynamic annealing of $\alpha$-quartz during Ne irradiations shows that the critical temperature above which no amorphization takes place is about 940 K. The activation energy for the diffusion of defects in the collision cascade or at the amorphous/crystalline interface is found to be 0.28 eV. The vacancy out-diffusion model is able to explain the experimental results well and the deduced critical temperature is close to the experimental value. The fluence for amorphization is independent of temperature up to about 550 K and then increases strongly with increasing temperature.

## ACKNOWLEDGMENTS

[1] M. Ohama, T. Fujiwara, and A. J. Ikushima, Appl. Phys. Lett. **73**, 1481 (1998).
[2] P. J. Chandler, F. L. Lama, P. D. Townsend, and L. Zhang, Appl. Phys. Lett. **53**, 89 (1988).
[3] P. D. Townsend, Nucl. Instrum. Methods Phys. Res. B **65**, 243 (1992).
[4] A. Nakajima, T. Futasugi, H. Nakao, T. Usuki, N. Horiguchi, and N. Yokoyama, Appl. Phys. Lett. **84**, 1316 (1998).
[5] F. Harbsmeier and W. Bolse, J. Appl. Phys. **83**, 4049 (1998).
[6] W. L. Gong, L. M. Wang, and R. C. Ewing, J. Appl. Phys. **84**, 4204 (1998).
[7] M. R. Pascucci, J. L. Hutchinson, and L. W. Hobbs, Radiat. Eff. **74**, 219 (1983).
[8] R. J. Macaulay Newcombe, D. A. Thompson, J. Davies, and D. V. Stevanovic, Nucl. Instrum. Methods Phys. Res. B **46**, 180 (1990).
[9] F. Priolo and E. Rimimi, Mater. Sci. Rep. **5**, 319 (1990).
[10] G. Götz, in *Ion Beam Modification of Insulators*, edited by P. Mazzoldi and G. W. Arnold (Elsevier, Amsterdam, 1987), p. 412.
[11] C. S. Marians and L. W. Hobbs, J. Non-Cryst. Solids **124**, 242 (1990).
[12] F. Roccaforte, W. Bolse, and K. P. Lieb, Appl. Phys. Lett. **73**, 1349 (1998).
[13] M. Uhrmacher, K. Pampus, F. G. Bergmeister, D. Purschke, and K. P. Lieb, Nucl. Instrum. Methods Phys. Res. B **9**, 234 (1985).
[14] J. Conrad, Ph.D. thesis, Universiät Göttingen, 1997.
[15] J. F. Biersack and J. M. Manoyan, Nucl. Instrum. Methods Phys. Res. B **35**, 215 (1988).
[16] W. Bolse, Mater. Sci. Eng., R. **12**, 53 (1994).
[17] W. Primak, Phys. Rev. B **6**, 4846 (1972).
[18] W. Bolse, Nucl. Instrum. Methods Phys. Res. B **141**, 133 (1998).
[19] S. U. Campisano, S. Coffa, V. Raineri, F. Priolo, and E. Rimini, Nucl. Instrum. Methods Phys. Res. B **80/81**, 514 (1993).
[20] F. F. Morehead and B. L. Crowder, Radiat. Eff. **6**, 27 (1970).
[21] S. X. Wang, L. M. Wang, and R. C. Ewing, J. Appl. Phys. **81**, 587 (1997).
[22] E. Wendler, T. Opfermann, and P. I. Gaiduk, J. Appl. Phys. **82**, 5965 (1997).